RSC Advances

PAPER

View Article Online
View Journal | View Issue

Cite this: *RSC Adv.*, 2017, **7**, 17403

Thermo-responsive fluorescence of AIE-active poly(*N*-isopropylacrylamides) labeled with highly twisted bis(*N*,*N*-dialkylamino)arenes†

Shunsuke Sasaki and Gen-ichi Konishi*

Received 27th January 2017
Accepted 13th March 2017

DOI: 10.1039/c7ra01212h

rsc.li/rsc-advances

Highly twisted bis(*N*,*N*-dialkylamino)arenes, which represent a new class of viscosity-sensitive fluorophores with aggregation-induced emission (AIE) luminogens, were introduced as co-monomers and cross-linkers into poly(*N*-isopropylacrylamides) (PNIPAMs). Despite the excellent performance of these bis(*N*,*N*-dialkylamino) arenes as fluorophores that are sensitive to the steric environment, synthetic methods to endow them with other reactive groups have not yet been reported. This study presents short synthetic pathways to 9,10-bis(*N*,*N*-dialkylamino)anthracenes (**BDAAs**) and 1,4-bis(*N*,*N*-dialkylamino)-2,3-dimethylnaphthalenes (**DMe-BDANs**) with hydroxyl groups at their alkyl chains. These hydroxyl groups were acylated to afford methacrylate moieties, which were subsequently used for the co-polymerization with *N*-isopropylacrylamide. At $T = 20$ °C, the resulting **BDAA**-containing PNIPAMs exhibited faint fluorescence ($\Phi_{fl} \approx 0.05$) in THF, whereas **DMe-BDAN**-containing PNIPAMs showed substantially stronger fluorescence in THF ($\Phi_{fl} \approx 0.32$) and water ($\Phi_{fl} \approx 0.55$) relative to the corresponding monomers. Moreover, **BDAA**-containing PNIPAMs featured a sharp increase of fluorescence intensity and quantum yield at $T = 27$–35 °C, while **DMe-BDAN**-containing PNIPAMs exhibited a continuous decrease of fluorescence intensity and Φ_{fl} with increasing temperature.

Introduction

Due to their sensitivity toward local viscosity, aggregation, and the binding to macromolecules, as well as their encapsulation in cavities, two types of fluorophores, *i.e.*, molecular rotors[1–5] and luminogens with aggregation-induced emission (AIEgens),[6–8] have received much attention regarding their fundamental and practical properties. Although various fluorescent molecular rotors and AIEgens have been developed, only few hold specific application monopolies. For example, in the area of molecular rotors, 9-(2-carboxy-2-cyano)vinyljulolidine (CCVJ) derivatives[1] have been extensively applied in molecular biology,[9,10] polymer science,[1,12] contact mechanics,[13] and fluid dynamics.[14] In the area of AIEgens, tetraphenylethene (TPE)[15] analogs are usually chosen in order to endow molecular systems with AIE functionality.[6,16] Given their simple structures and facile functionalization, it is hardly surprising that CCVJs and TPEs were easily incorporated into larger, more elaborate molecular systems.[1,10,12,13,16] From a practical perspective, it is thus very important that novel fluorophores with improved photophysical properties also exhibit the potential for facile subsequent functionalization.[17]

Some of our previous experimental and theoretical studies revealed that highly twisted *N*,*N*-dialkylamino groups at the *para*-positions of typical aromatic hydrocarbons induce AIE and viscosity-responsive fluorescence.[18] This general design strategy enabled us to develop structurally simple AIEgens such as 9,10-bis(*N*,*N*-dialkylamino)anthracenes (**BDAAs**) and 1,4-bis(*N*,*N*-dialkylamino)-2,3-dimethylnaphthalenes (**DMe-BDANs**). In addition to their acute viscosity-responsiveness, **BDAAs** and **DMe-BDANs** feature brighter solid-state fluorescence compared to other simple AIEgens.[18,19] Therefore, **BDAAs** and **DMe-BDANs** represent promising prospectives for microenvironmental probes. However, synthetic routes to highly twisted bis(*N*,*N*-dialkylamino) arenes with functional groups at their alkyl chains have not yet been reported, despite the fact that numerous studies have been reported regarding the synthesis of sterically congested *N*,*N*-diarylaminoarenes.[20,21]

Herein, we present a facile route to functionalize the alkyl chains of **BDAAs** and **DMe-BDANs**. These compounds were subsequently used as co-monomers and cross-linkers in the polymerization of *N*-isopropylacrylamides, which afforded the corresponding poly(*N*-isopropylacrylamides) (PNIPAMs). In aqueous solution, PNIPAMs undergo a coil-to-globule transition at $T \approx 31$ °C.[22] While the phase transition itself has been the subject of extensive research, the sharp phase-transition behavior close to the lower critical solution temperature (LCST) has been used to visualize intracellular temperature.[23] For both fundamental and practical purposes, various fluorophores such

Department of Chemical Science and Engineering, Tokyo Institute of Technology, O-okayama, Meguro-ku, Tokyo, 152-8552, Japan. E-mail: konishi.g.aa@m.titech.ac.jp; Fax: +81-3-5734-2888; Tel: +81-3-5734-2321

† Electronic supplementary information (ESI) available: ^{1}H and ^{13}C NMR charts, and data of photophysical studies. See DOI: 10.1039/c7ra01212h

as pyrene,[24] 3-hydroxyflavone,[25] benzofurazan,[26] rhodamine,[27] and BODIPY[28] have been introduced into PNIPAMs. In the same way, PNIPAMs containing **BDAAs** and **DMe-BDANs** should be expected to act as a microenvironmental probes. Furthermore, **BDAAs** and **DMe-BDANs** exhibit not only AIE but also viscosity-sensitive fluorescence. These fluorophores should therefore most likely be able to visualize weak restrictions of intramolecular motions (RIM), which result from specific interactions between PNIPAM chains, fluorophores, and H_2O molecules, in addition to the severe RIM imposed by a coil-to-globule transition of the PNIPAM chains. Herein, we report the temperature-dependent fluorescence behavior of **BDAA**- and **DMe-BDAN**-labeled PNIPAMs and the corresponding gels.

Results and discussion

Synthesis of bis(*N*,*N*-dialkylamino)arenes functionalized at their alkyl chains

The syntheses of 9,10-bis((*N*-(3′-(*N*″-(3″-hydroxyprop-1″-yl)-*N*″-methylamino))prop-1′-yl)-*N*-methylamino)anthracene (**6**) and 1,4-bis(*N*-(hydroxypent-5-yl)-*N*-methylamino)-2,3-dimethyl naphthalene (**14**) with hydroxy groups at the terminal positions of their alkyl chains are outlined in Schemes 1 and 2, respectively. The hydroxyl groups in **6** and **14** were subsequently transformed into methacrylate moieties in order to prepare fluorescent monomers (**ANTH-monomer** and **NAPH-monomer**) and cross-linkers (**ANTH-linker** and **NAPH-linker**). Detailed synthetic procedures are described in the Experimental section. Alcoholamines, especially those with straight-chain structures, have been reported to deactivate palladium/phosphine catalyst systems by chelating palladium.[29] For the *N*-arylation of alcoholamines, the copper iodide/2-isobutyrylcyclohexane system has been proposed as an alternative.[30,31] However, a catalyst test on the coupling between 1-bromo-iodonaphthalene and 5-amino-1-pentanol revealed that this system yielded only trace amounts of the desired product. Therefore, the nucleophilicity of the hydroxyl group on the alcoholamine should be disabled prior to the C–N coupling. This may be accomplished by either functional group interconversion (FGI)[32] or by protection–deprotection strategies.[33,34]

For the synthesis of terminal-functionalized 9,10-bis(*N*,*N*-dialkylamino)anthracene **6**, the same catalyst system was employed as for the formation of the highly twisted *N*,*N*-dialkylaminoarenes,[18,19] *i.e.*, Pd-PEPPSI-IPr.[20,35] As 9,10-diaminoanthracene and its *N*-monoalkylated derivatives are extremely sensitive to oxydation,[18,36] a secondary amine (**2**) was chosen as the coupling partner for 9,10-dibromoanthracene (**1**). Subsequently, the chloride atoms in **3** were replaced with bromide atoms[37] in order to enhance the reactivity toward a subsequent S_{N2} reaction with alcoholamine **5**. The S_{N2} reaction proceeded selectively on the amine moiety to afford **6**, which was confirmed by NOEs around the *N*-methyl group (Fig. S5†). In addition, functionalization with a methacrylate moiety endowed the resulting compounds with the characteristic absorption at 1717 cm^{-1}, which clearly indicates the formation of an ester instead of an amide group. The overall yield of **6** with respect to starting material **1** was 53%.

For the naphthalene-based system, a protection–deprotection strategy was employed in order to introduce hydroxyl groups at the terminal positions of the alkyl chains (Scheme 2). In this case, a route similar to Scheme 1 cannot be applied, as the secondary amine cannot be introduced at the 1- and 4-positions of 1,4-dibromo-2,3-dimethylnaphthalene by C–N coupling reactions.[18] Furthermore, an FGI strategy as outlined in Scheme 1 would be more laborious than that described in Scheme 2. Firstly, 2,3-dimethylnaphthalene (**8**) was regioselectively brominated to give **9**.[38] Subsequently, **9** was combined with *tert*-butyldiphenylsilyl (TBDPS)-protected 5-amino-1-pentanol **11**. It should be noted here that the C–N coupling between **9** and **11** proceeded successfully in the presence of trace amounts of moisture on the glass vessel, while the product yield was poor in the absence of moisture within the vessel after *e.g.* flame-drying *in vacuo*. The subsequent permethylation did not require adherence to strict stoichiometry between **13** and methyl iodide as the substantial steric hindrance around the nitrogen atoms prevents the further methylation of the tertiary amine moiety, even in the presence of an excess of methyl iodide. A final deprotection of the TBDPS group afforded **14** in 65% overall yield relative to 2,3-

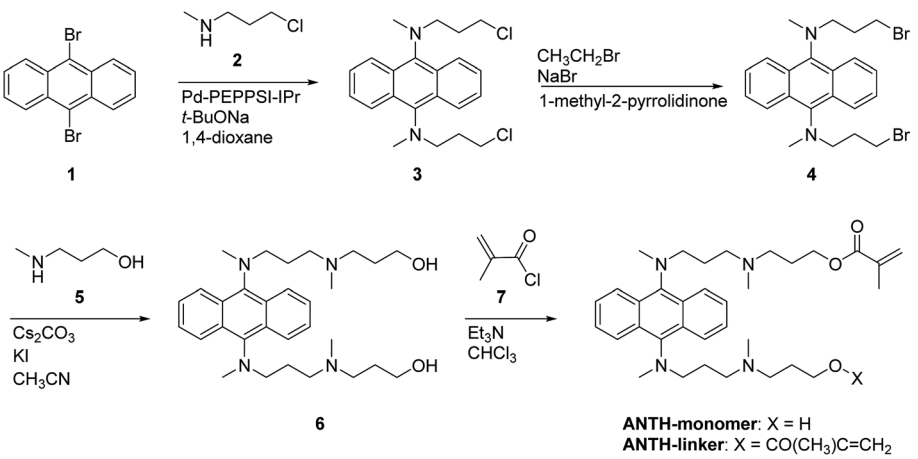

Scheme 1 Synthetic route to terminal-functionalized 9,10-bis(*N*,*N*-dialkylamino)anthracenes.

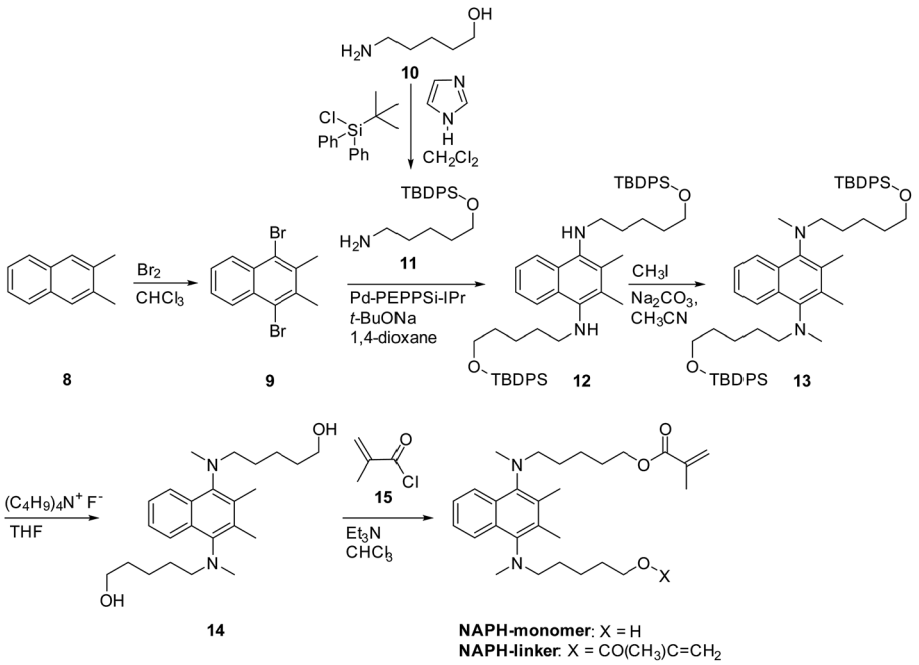

Scheme 2 Synthetic route to terminal-functionalized 1,4-bis(*N*,*N*-dialkylamino)-2,3-dimethylnaphthalenes.

dimethylnaphthalene (**8**). The ^{1}H and ^{13}C NMR spectra of **14** showed pairs of peaks with comparable chemical shifts, identical peak multiplicities, and coupling constants (Fig. S14 and S15†). Further NMR studies based on DEPT-135, ^{1}H–^{1}H COSY, and ^{1}H–^{13}C HSQC techniques allowed a complete assignment of these peaks (Fig. S15–S17†). Variable-temperature (VT) NMR experiments revealed that these pairs of peaks originate from an equilibrium of two conformers (Fig. 1),[39] while chemical-exchange peaks could not be discerned from the diagonal peaks in the NOESY spectra (Fig. S18†).[40] These conformers are in fact two rotamers, which differ with respect to the rotation around the aryl-N bonds (Fig. 2a and b). As illustrated in Fig. 2c, the NOE signal of the H_h and $H_{h'}$ protons (1.59–1.49 ppm) intensified upon irradiating one of the H_f protons (2.93 ppm). In contrast to the *cis*-rotamer, the H_f protons in the *trans*-rotamer should be in close spatial proximity to both H_h and $H_{h'}$ protons (Fig. 2a and b). The observed stronger NOE for H_h and $H_{h'}$ thus indicates that the irradiated H_f proton peak should be attributed to the *trans*-rotamer. The slow equilibrium between the two rotamers on the NMR timescale reflects the severe steric restrictions imposed by the *peri*-hydrogen atoms and methyl groups at the 2- and 3-positions of the naphthalene core.

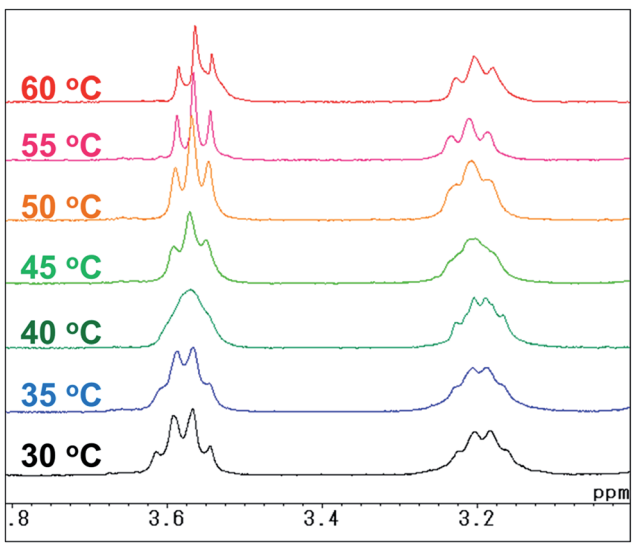

Fig. 1 Variable-temperature ^{1}H NMR spectra (300 MHz, $CDCl_3$) of 1,4-bis(*N*-(hydroxypent-5-yl)-*N*-methylamino)-2,3-dimethylnaphthalene (**14**).

Co-polymerization of *N*-isopropylacrylamide with bis(*N*,*N*-dialkylamino)arene-based monomers and cross-linkers

As outlined in Scheme 3, **ANTH-monomer** and **NAPH-monomer** were co-polymerized using various monomer feed ratios (x : y) to afford co-polymers **[ANTH-polymer]**$_x$ (yields: 61–84%) and **[NAPH-polymer]**$_x$ (yields: 91–96%). The thus obtained copolymers were purified by repeated reprecipitation into diethyl ether (for details, see the Experimental section). The ^{1}H NMR spectra of **[ANTH-polymer]**$_x$ and **[NAPH-polymer]**$_x$ (Fig. S23 and S24†) are consistent with those previously reported for PNIPAMs,[41] except for the small signals of the fluorophore moieties. Weight-average molecular weights (M_w) and polydispersity indexes (M_w/M_n; PDI) were determined by size exclusion chromatography (SEC; Fig. S25 and S26†). In general, **[ANTH-polymer]**$_x$ exhibited smaller M_w values and broader polydispersity values (M_w = 48 000–66 000 g mol^{-1}, M_w/M_n = 2.51–2.61) than **[NAPH-polymer]**$_x$ (M_w = 65 000–80 000 g mol^{-1}, M_w/M_n = 2.25–2.37). The copolymer composition m : n (Scheme 3) was calculated from the corresponding UV-Vis spectra. For that purpose, molar

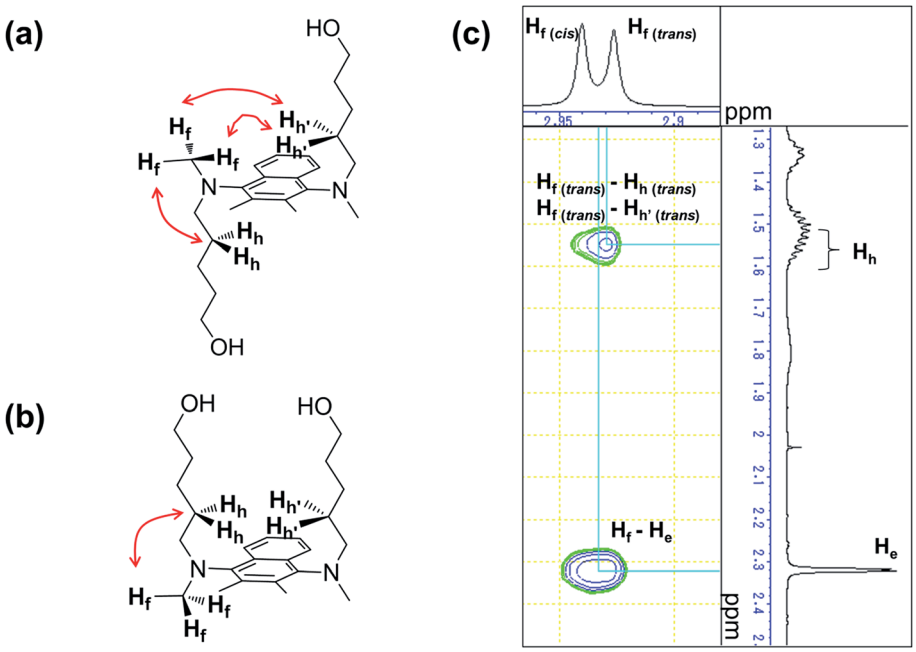

Fig. 2 Chemical structure of the (a) *trans*- and the (b) *cis*-rotamer of 1,4-bis(*N*-(hydroxypent-5-yl)-*N*-methylamino)-2,3-dimethylnaphthalene (**14**) (red arrows represent NOE signals). (c) NOESY spectrum (500 MHz, $CDCl_3$) of **14** for the H_f peak area.

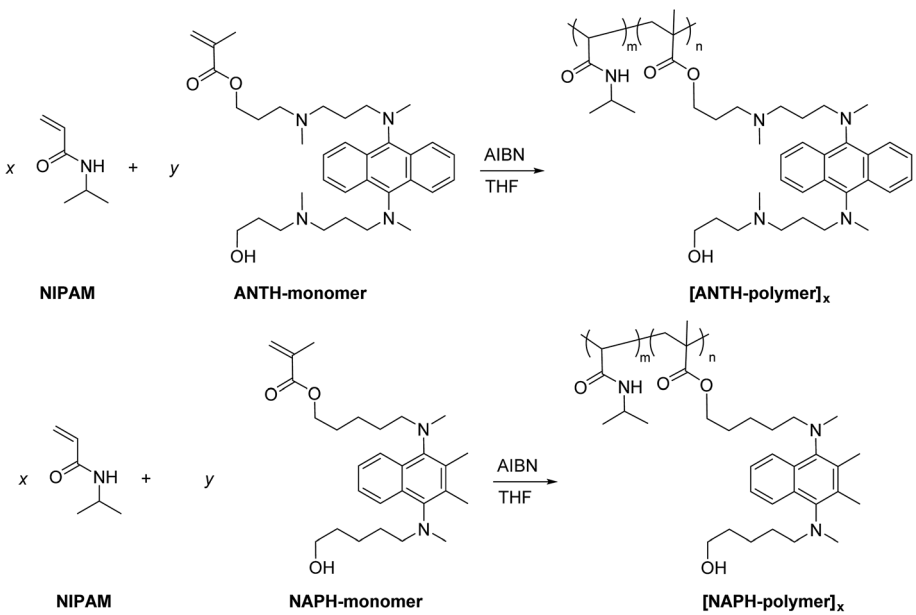

Scheme 3 Co-polymerization of *N*-isopropylacrylamide with **ANTH-monomer** and **NAPH-monomer**.

absorption coefficients of **6** ($\varepsilon = 5330\ M^{-1}\ cm^{-1}$ at $\lambda_{abs} = 401$ nm) and **14** ($\varepsilon = 2700\ M^{-1}\ cm^{-1}$ at $\lambda_{abs} = 321$ nm) were derived from calibration lines (Fig. S27†), and used to determine the concentration of the fluorophore moieties. While the $m : n$ ratio of the **[NAPH-polymers]**$_x$ agreed well with the monomer feed ratio $x : y$, the concentration of the fluorophore moieties in **[ANTH-polymer]**$_x$ was significantly lower than expected (Table 1). Considering that the relative reactivity of **ANTH-monomer** and **NAPH-monomer** should be comparable, the physical properties of the **ANTH-monomer**, such as incompatibility with concentrated PNIPAMs, may be responsible for the lower molecular weight, the broader polydispersity, and the inefficient incorporation of the fluorophore moieties.

Under the same conditions used for the preparation of **[ANTH-polymer]**$_x$ and **[NAPH-polymer]**$_x$, **[ANTH-gel]**$_x$ and **[NAPH-gel]**$_x$ were prepared by free-radical polymerizations (Scheme 4). In a preliminary experiment, the co-polymerization was examined for a monomer concentration of 1.0 M, using

Table 1 Monomer feed ratios (x : y), copolymer compositions (m : n), weight-average molecular weights (M_w), and polydispersity indexes (M_w/M_n) for **[ANTH-polymer]**$_x$ and **[NAPH-polymers]**$_x$

Entry	x : y	m : n[a]	M_w[b] [g mol^{-1}]	M_w/M_n[b]
[ANTH-polymer]$_{167}$	167 : 1	180 : 1	48 000	2.54
[ANTH-polymer]$_{83}$	83 : 1	90 : 1	66 000	2.61
[ANTH-polymer]$_{56}$	56 : 1	84 : 1	53 000	2.51
[NAPH-polymer]$_{167}$	167 : 1	169 : 1	65 000	2.25
[NAPH-polymer]$_{83}$	83 : 1	83 : 1	76 000	2.30
[NAPH-polymer]$_{56}$	56 : 1	56 : 1	80 000	2.37

[a] Co-polymer composition based on the UV-Vis spectra (Fig. S27). [b] Molecular weight and PDI based on SEC (DMF + 0.01 M LiBr) using calibrations with polystyrene standards.

varying monomer feed ratios ($x : y$ = 333 : 1, 167 : 1, and 83 : 1; Table 2). However, the preliminary experiment did not afford infusible and/or insoluble gels. Therefore, the monomer concentration (2.5 M) and the molar ratio of cross-linkers were increased ($x : y$ = 167 : 1, 83 : 1 and 56 : 1). These changes successfully furnished PNIPAM gels **ANTH-linker** and **NAPH-linker** (see the Experimental section). The thus obtained PNIPAM gels were swollen in water and THF and their swelling ratio was consistent with the molar ratio of the cross-linkers (Table 2). Therefore, it can be concluded that **ANTH-linker** and **NAPH-linker** were successfully introduced as cross-linkers in the PNIPAM gels.

Photophysical properties of [ANTH-polymer]$_x$ and [ANTH-gel]$_x$

The absorption and fluorescence spectra, as well as the fluorescence quantum yields (Φ_{fl}) of **ANTH-monomer** and **ANTH-linker** were recorded in *n*-hexane, THF, acetonitrile, and methanol. A summary of the data is compiled in Fig. S28 and S29 and Table S1,† while data measured in THF are listed in Table 3 and Fig. 3. **ANTH-monomer** and **ANTH-linker** exhibited almost identical absorption and fluorescence spectra. These photophysical properties are comparable to those of **BDAAs** without functionalization at the alkyl chains.[18] It can thus be concluded that the functionalization of alkyl chains of **BDAAs** does not affect their photophysical properties. Regardless of the monomer feed ratio $x : y$, **[ANTH-polymer]**$_x$ showed in both THF and aqueous solution identical absorption and fluorescence spectra as well as Φ_{fl} values (Table 3 and Fig. S30†). The spectra of **[ANTH-polymer]**$_x$ are similar to those of **ANTH-monomer** and **ANTH-linker**, except for the deviation of the absorption spectrum at λ_{abs} = ~300 nm, which should be attributed to the absorption of PNIPAM.[42] In aqueous solution, **[ANTH-polymer]**$_x$ exhibited a broader absorption band, a slight bathochromic shift of the fluorescence spectrum (Fig. 3), and enhanced Φ_{fl} (Table 2) than in THF solution. Although both THF and water represent good solvents for PNIPAM, the solvation mechanism for PNIPAM in water is substantially different from that in THF, and results in restricted motion of the side chains.[43,44] Moreover, the hydrophobicity of the fluorophores[45,46] and the relatively high viscosity[47] of pure water most likely contribute to the enhanced Φ_{fl}. Similarly, the Φ_{fl} of **[ANTH-gel]**$_x$ increased upon swelling in water (0.20–0.24), while those of **[ANTH-gel]**$_x$ swollen in THF were comparable to those of **ANTH-monomer** and **[ANTH-polymer]**$_x$ in THF (Table 2). According to the swelling ratios, the concentration of PNIPAM and cross-linkers in swollen **[ANTH-gel]**$_x$ was much higher than in an aqueous

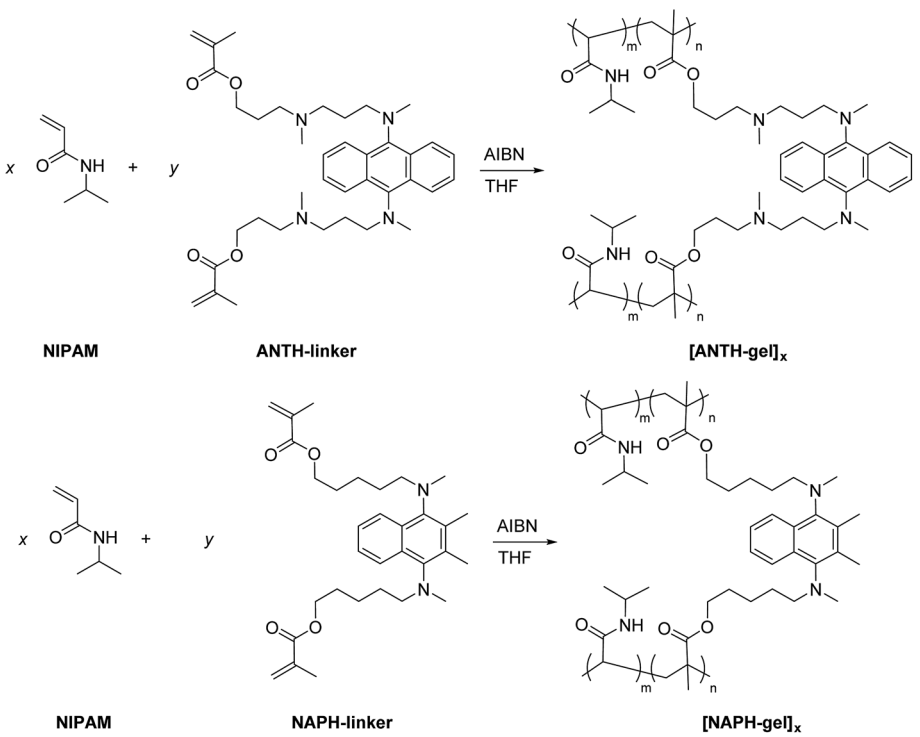

Scheme 4 Co-polymerization of *N*-isopropylacrylamide with ANTH-linker and NAPH-linker.

Table 2 Experimental conditions for the preparation of the gels,[a] swelling ratios [$(W' - W)/W$], as well as fluorescence quantum yields (Φ_{fl}) for the dried gels and those swollen in water and THF

Entry	Monomer [M]	$x : y$	Swelling ratio $(W' - W)/W$[b]	Φ_{fl} (dried)	Φ_{fl} (H_2O)[c]	Φ_{fl} (THF)[d]
[ANTH-gel]$_{333}$	1.0	333 : 1	No gelation (pale yellow powder)			
[ANTH-gel]$_{167}$	1.0	167 : 1	No gelation (pale yellow powder)			
[ANTH-gel]$_{83}$	1.0	83 : 1	No gelation (pale yellow powder)			
[ANTH-gel]$_{167}$	2.5	167 : 1	No gelation (yellow viscous liquid)			
[ANTH-gel]$_{83}$	2.5	83 : 1	14.2	0.24	0.22	0.07
[ANTH-gel]$_{56}$	2.5	56 : 1	3.57	0.21	0.20	0.05
[NAPH-gel]$_{167}$	2.5	167 : 1	17.1	0.52	0.53	0.33
[NAPH-gel]$_{83}$	2.5	83 : 1	4.43	0.46	0.47	0.28
[NAPH-gel]$_{56}$	2.5	56 : 1	2.87	0.49	0.53	0.28

[a] 1.0 mol% AIBN, THF, $T = 55$ °C, $t = 20$ h. [b] W: weight of the dry gel; W': weight of the gel swollen in water. [c] Immersed in water for 48 h. [d] Immersed in THF for 48 h.

Table 3 Photophysical parameters for **ANTH-monomer**, **ANTH-linker**, and **[ANTH-polymer]$_x$** (x = 56, 83, 167)[a]

Entry	Solvent	$x : y$	λ_{abs} [nm]	λ_{fl}[b] [nm]	Φ_{fl}[b]
ANTH-monomer	THF	—	400	527	0.05
ANTH-linker	THF	—	400	526	0.05
[ANTH-polymer]$_x$	THF	167 : 1	401	526	0.05
	THF	83 : 1	401	525	0.05
	THF	56 : 1	401	526	0.05
	H_2O	167 : 1	403	531	0.09
	H_2O	83 : 1	403	529	0.11
	H_2O	56 : 1	403	529	0.11

[a] All measurements were conducted at $T = 20$ °C. [b] Excitation wavelength corresponds to the maximum of the first absorption band λ_{abs}.

solution of **[ANTH-polymer]$_x$** (1 g L^{-1}), which would explain the high Φ_{fl} observed for **[ANTH-gel]$_x$** swollen in water.

[ANTH-polymer]$_{167}$ exhibited the large enhancement of fluorescence intensity and Φ_{fl} at $T = 27$–35 °C (Fig. 4). Upon heating, the relative fluorescence intensity (I/I_0) initially increased at $T = 27$–28 °C and peaked at $T = 33$–35 °C. Further heating led to a rapid decrease of I/I_0 and at $T = 50$ °C, I/I_0 fell below unity ($T = 21$ °C). A similar behavior of I/I_0 was also observed for other monomer feed ratios $x : y$ (Fig. S34†). This fluctuation of I/I_0 coincided with the coil-to-globule transition of the PNIPAM chains;[22] the transmittance of the **[ANTH-polymer]$_x$** solutions began to decrease at $T = 28$ °C and finished at $T = 40$–45 °C (Fig. S32†). Peaking of I/I_0, accompanied by a coil-to-globule transition of the polymer chains has been reported for some cases of fluorophore-labeled PNIPAM-based polymers[27,48,49] and their microgels,[50] although a decrease of fluorescence intensity at higher temperature is usually insignificant in diluted solution (≈0.01–0.02 g L^{-1}).[51,52] The Φ_{fl} values for **[ANTH-polymer]$_x$** (Fig. 4b and S34†) showed a far less drastic decrease even at higher temperatures. Therefore, fast internal conversion or any other thermally induced deactivation processes should be insignificant for the decrease of I/I_0. Given that the fluorescence intensity is a function of Φ_{fl} and the absorbance, the main reason for the decrease of I/I_0 at higher temperatures should be associated with the less efficient absorption of the excitation light at $T > 35$ °C. This should be due to the aggregation of dehydrated **[ANTH-polymer]$_x$** at higher temperature and a concomitantly high heterogeneity of

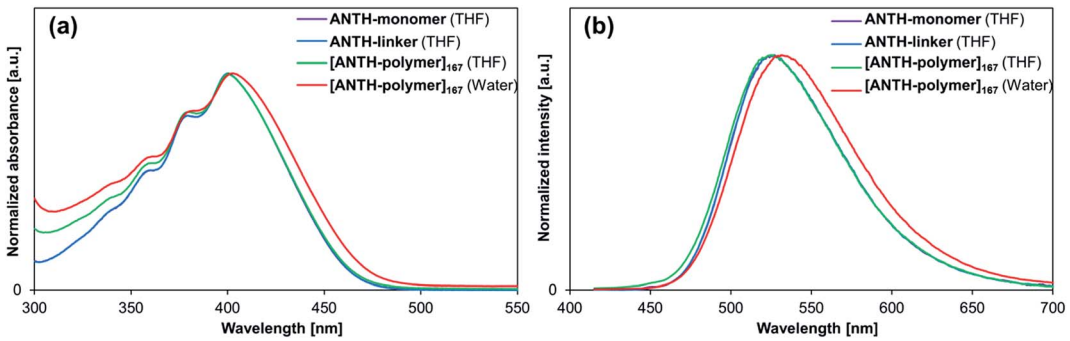

Fig. 3 (a) Absorption and (b) fluorescence spectra of **ANTH-monomer** (purple), **ANTH-linker** (blue), and **[ANTH-polymer]$_{167}$** in THF (green), as well as of **[ANTH-polymer]$_{167}$** in water (red).

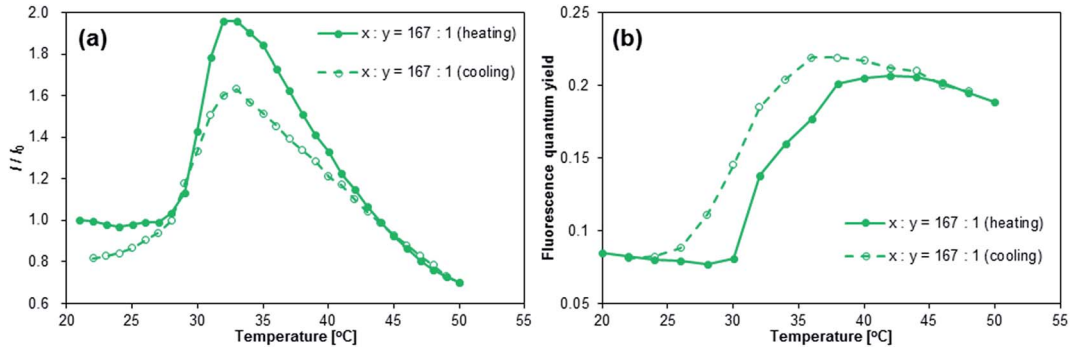

Fig. 4 Temperature dependence of (a) the fluorescence intensity (I) and (b) fluorescence quantum yields (Φ_{fl}) of **[ANTH-polymer]**$_{167}$; I_0 = fluorescence intensity at ~530 nm; T = 21 °C, λ_{ex} = 403 nm, and c_{solute} = 1 g L^{-1}.

the solution, through which the bulk of the excitation light could pass or be scattered from without absorption.

Even though the peaking of I/I_0 was also observed during the cooling, it was less pronounced than during the heating. In addition, Φ_{fl} exhibited a "hysteresis"-type behavior, *i.e.*, the Φ_{fl} of **[ANTH-polymer]**$_x$ remained higher during the cooling than during the heating, but both values coincided eventually at T = 22 °C. In fact, the temperature-dependent transmittance (Fig. S32†) of **[ANTH-polymer]**$_{167}$ during the cooling is almost identical to that during the heating. Therefore, the two hystereses observed during cooling should be attributed to microenvironments around the fluorophores rather than to abnormalities of the LCST behavior of **[ANTH-polymer]**$_x$. As far as I/I_0 is concerned, the heterogeneity of the optical density should be responsible for the observed hysteresis; immediately after hydration, the polymer chains should be in close spatial proximity with respect to each other, and consequently, absorption of the excitation lights should be inefficient. Higher Φ_{fl} values during the cooling should be ascribed to restrictions of the intramolecular motion of the fluorophores that persisted up to a late stage of hydration.

[ANTH-gel]$_x$ also exhibited an increase of Φ_{fl} at T = 25–32 °C (Fig. 5a). However, the increase of Φ_{fl} is less than half of that of **[ANTH-polymer]**$_x$, which is due to the fact that **[ANTH-gel]**$_x$ is already fluorescent at T = 20 °C (Φ_{fl} = 0.20–0.22). Further heating (T > 32 °C) induced a significant decrease of Φ_{fl}, resulting in a peak of Φ_{fl} at $T \approx$ 32 °C. In the measurements of both **[ANTH-gel]**$_x$ and **[NAPH-gel]**$_x$, experimental errors were inevitable due to the limited absorbance of these gel samples. At this stage, we are unable to unequivocally determine the cause of the decrease of Φ_{fl} at T > 32 °C, but the results nevertheless demonstrate that **BDAA** can be used to probe the coil-to-globule transition of the PNIPAM chains.

Photophysical properties of [NAPH-polymer]$_x$ and [NAPH-gel]$_x$

Absorption and fluorescence spectra, as well as Φ_{fl} values and fluorescence lifetimes were examined for **NAPH-monomer** and **NAPH-linker** in polar and nonpolar solvents (Table S1 and Fig. S31†). The photophysical parameters obtained from THF solutions are summarized in Table 4. Although the absorption and fluorescence spectra of **NAPH-monomer** and **NAPH-linker** were almost identical (Fig. 6), their Φ_{fl} values in THF were significantly higher (Φ_{fl} = 0.14–0.20) than that of **DMe-BDAN** (Φ_{fl} = 0.04).[18] This difference may be attributed to the flexible alkyl chain of **NAPH-monomer** and **NAPH-linker**; our previous study suggested that flexible alkyl chains could induce planarity around the aryl-N bonds of *N*,*N*-dialkylaminoarenes, which may result in relatively large oscillator strengths for the $S_0 \leftarrow {}^1CT$ fluorescence transition.[18] The co-polymerization or cross-linking with NIPAM resulted in a further increase of the Φ_{fl} for **[NAPH-polymer]**$_x$ in THF (Φ_{fl} = 0.32–0.34) and in H_2O (Φ_{fl} = 0.54–0.59), as well as for **[NAPH-gel]**$_x$ in THF (Φ_{fl} = 0.28–0.33)

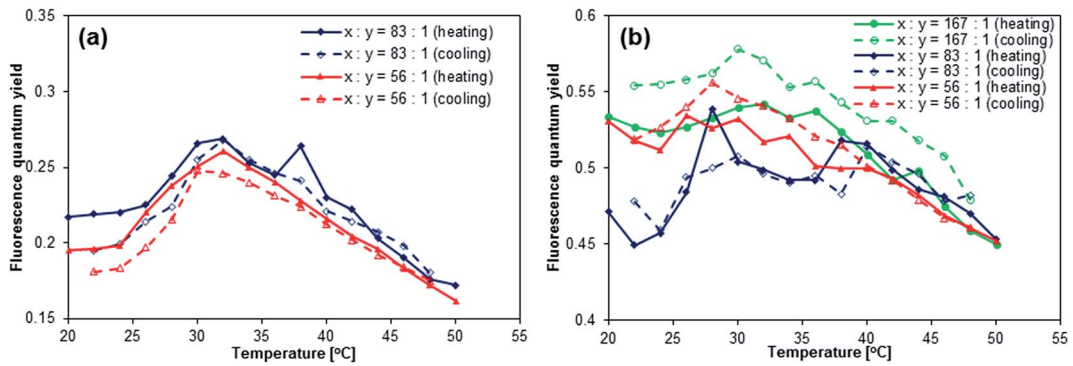

Fig. 5 Temperature dependence of the fluorescence quantum yields of (a) **[ANTH-gel]**$_{83}$ (blue) and **[ANTH-gel]**$_{56}$ (red) in H_2O (λ_{ex} = 403 nm) and (b) **[NAPH-gel]**$_{167}$ (green), **[NAPH-gel]**$_{83}$ (blue), and **[NAPH-gel]**$_{56}$ (red) in H_2O (λ_{ex} = 323 nm).

Table 4 Photophysical parameters of **NAPH-monomer**, **NAPH-linker**, and **[NAPH-polymer]$_x$** (x = 56, 83, 167)[a]

Entry	Solvent	x : y	λ_{abs} [nm]	λ_{fl}[b] [nm]	Φ_{fl}[b]	τ_{fl}[c] [ns]
NAPH-monomer	THF	—	320	432	0.20	2.94
NAPH-linker	THF	—	318	430	0.14	2.33
[NAPH-polymer]$_x$	THF	167 : 1	318	430	0.32	3.26 (0.25) 5.80 (0.75)
	THF	83 : 1	320	430	0.32	3.83 (0.47) 6.29 (0.53)
	THF	56 : 1	320	432	0.34	3.75 (0.42) 6.21 (0.58)
	H_2O	167 : 1	324	442	0.54	—
	H_2O	83 : 1	322	439	0.58	—
	H_2O	56 : 1	323	436	0.59	—

[a] All measurements conducted at T = 20 °C. [b] Excitation wavelength corresponds to the maximum of the first absorption band λ_{abs}. [c] λ_{ex} = 343 nm.

and H_2O (Φ_{fl} = 0.47–0.53). The relatively high Φ_{fl} value observed for **[NAPH-polymer]$_x$** in THF coincides with the emergence of a long-lived excited-state species ($\tau_{fl} \approx 6$ ns), which indicates specific interactions between the PNIPAM chains and the fluorophore. However, considering the structural differences between **NAPH-monomer** and **ANTH-monomer**, *i.e.*, shorter side chains, a smaller π-system, and the absence of aliphatic amino groups, it is difficult to determine precisely how the fluorophores in **[NAPH-polymer]$_x$** interact with the PNIPAM chains in THF.

Given that the aqueous solutions of **[NAPH-polymer]$_x$** are already fluorescent at T = 20 °C, the relative fluorescence intensity I/I_0 declined during heating (Fig. 7a and S35†). Even though a small increase of Φ_{fl} at T = 30–35 °C was observed for **[NAPH-polymer]$_{167}$** (Fig. 7b), the Φ_{fl} of **[NAPH-polymer]$_x$** (x = 56, 83) also decreased with increasing temperature (Fig. S35†). It should also be noted that the temperature-dependent transmittance of **[NAPH-polymer]$_x$**, monitored at 650 nm, was largely affected by the incorporation of the fluorophore (Fig. S33†). For **[NAPH-polymer]$_x$**, the decrease of transmittance occurred much slower and persisted up to higher temperatures than that of pristine PNIPAM.[53] Especially **[NAPH-polymer]$_x$** (x = 56 and 83) exhibited a steep drop of the transmittance, even at T > 40 °C. It has previously been reported that small amounts of hydrophobic moieties substantially affect the LCST behavior of the PNIPAM chains.[45,48] Considering that the fluorophores in **[NAPH-polymer]$_x$** is subject to specific interactions with the PNIPAM chains even in THF, it is reasonable to expect a severe perturbation of the LCST behavior of **[NAPH-polymer]$_x$**. Similar to the Φ_{fl} of **[NAPH-polymer]$_x$**, that of **[NAPH-gel]$_x$** did not show any temperature dependence (Fig. 5b), *i.e.*, although the Φ_{fl} of **[NAPH-gel]$_x$** declined slightly with increasing temperature, the signal-to-noise ratio was too low to discern any reliable trends.

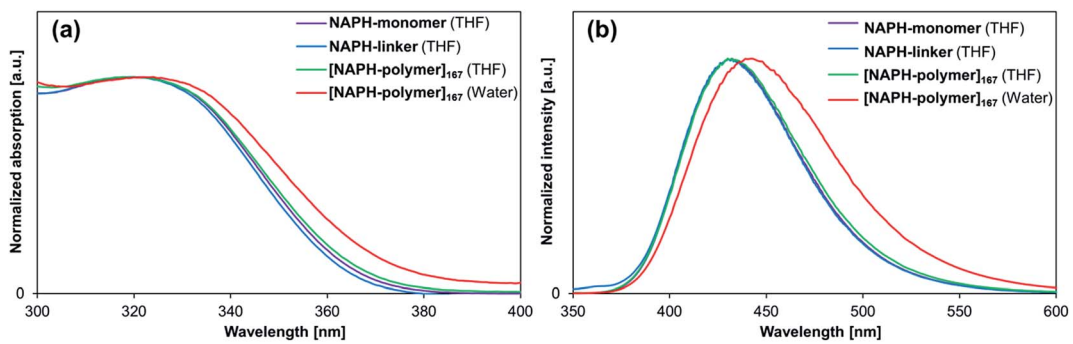

Fig. 6 (a) Absorption and (b) fluorescence spectra of **NAPH-monomer** (purple), **NAPH-linker** (blue), and **[NAPH-polymer]$_{167}$** (green) in THF, as well as of **[NAPH-polymer]$_{167}$** in H_2O (red).

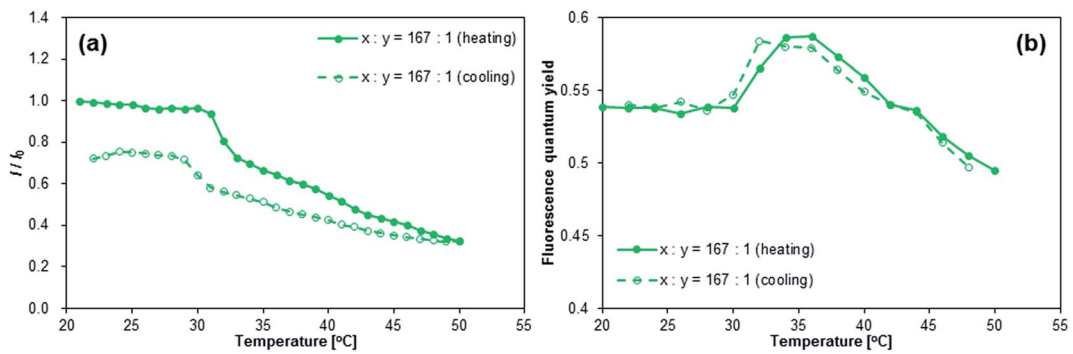

Fig. 7 Temperature dependence of (a) the fluorescence intensity (I) and (b) fluorescence quantum yields (Φ_{fl}) of **[NAPH-polymer]$_{167}$**; I_0 = fluorescence intensity at ~440 nm; T = 21 °C, λ_{ex} = 323 nm, and c_{solute} = 1 g L^{-1}.

Conclusions

In this study, we presented the synthesis of 9,10-bis((*N*-(3′-(*N*″-(3″-hydroxyprop-1″-yl)-*N*″-methylamino))prop-1′-yl)-*N*-methylamino) anthracene (**6**) and 1,4-bis(*N*-(hydroxypent-5-yl)-*N*-methylamino)-2,3-dimethylnaphthalene (**14**), which contain hydroxy groups at the terminal positions of their alkyl chains. While the former was obtained in 53% yield from a three-step protocol, the latter required four steps (yield: 65%). Due to the severe steric hindrance imposed by the *peri*-hydrogen and methyl groups at the 2- and 3-positions of **14**, two rotamers with respect to the aryl-N bonds were observed. After endowing **6** and **14** with methacrylate moieties, **ANTH-monomer**, **ANTH-linker**, **NAPH-monomer**, and **NAPH-linker** were used for co-polymerizations with *N*-isopropylacrylamide to afford fluorophore-labeled PNIPAMs and the corresponding gels. While **[ANTH-polymer]**$_x$ exhibited low fluorescence, similar to **ANTH-monomer** and **ANTH-linker**, THF solutions of **[NAPH-polymer]**$_x$ exhibited stronger fluorescence ($\Phi_{fl} = 0.32$–0.34) than those of **NAPH-monomer** and **NAPH-linker** ($\Phi_{fl} = 0.14$–0.20); in aqueous solution, the fluorescence quantum yields of **[NAPH-polymer]**$_x$ increased even further ($\Phi_{fl} = 0.54$–0.59). In a similar manner, **[ANTH-gel]**$_x$ was only weakly fluorescent in THF ($\Phi_{fl} = 0.05$–0.07), while the fluorescence of **[NAPH-gel]**$_x$ was stronger in THF ($\Phi_{fl} = 0.28$–0.33). The temperature-dependent fluorescence of **[ANTH-polymer]**$_x$ and **[ANTH-gel]**$_x$ revealed a steep increase of fluorescence intensity and Φ_{fl} at $T = 27$–35 °C, while **[NAPH-polymer]**$_x$ and **[NAPH-gel]**$_x$ did not exhibit an increase in fluorescence intensity upon heating. Thus, 9,10-bis(*N*,*N*-dialkylamino)anthracene (**BDAA**) is able to act as a useful probe for the microenvironment of PNIPAM chains In contrast, the sensitivity of 1,4-bis(*N*,*N*-dialkylamino)-2,3-dimethylnaphthalene (**DMe-BDAN**) toward the steric environment was hindered by interactions with the PNIPAM chains. Nevertheless, **DMe-BDAN** may be used to monitor other aspects of microenvironments, *e.g.* the local viscosity or molecular mobilities, upon introduction into suitable systems without such interactions.[18] This study thus provides access to terminal-functionalized **BDAA** and **DMe-BDAN**, and these may be subjected to further modifications in order to facilitate their incorporation into larger and more complex molecular systems. Given their sensitivity and versatility, we expect these fluorophores to find a multitude of applications.

Experimental procedure

Variable-temperature photophysical studies

Unless otherwise noted, all measurements were conducted under ambient conditions and temperature ($T = 293$ K). For the photophysical measurements in THF, the solute concentration of **[ANTH-polymer]**$_x$ and **[NAPH-polymer]**$_x$ were adjusted so that the optical density (O.D.) at the maximum of the first absorption band was 0.1. For the variable-temperature photophysical measurements, aqueous solutions of **[ANTH-polymer]**$_x$ and **[NAPH-polymer]**$_x$ ($c_{solute} = 1$ g L^{-1}) were prepared and aliquots of 3.5 mL were transferred into quartz cells (1 cm). The samples of **[ANTH-gel]**$_x$ and **[NAPH-gel]**$_x$ used for the photophysical measurements were prepared by dipping ϕ 6 mm × 22 mm glass tubes in the co-polymerization reaction mixtures (for details, see the synthetic procedure), yielding cylindrical gels (ϕ 4 mm × 15 mm) after drying. These cylindrical gel samples were transferred into quartz cells (1 cm × 1 cm) and immersed in THF or water for 48 h. Immediately prior to the photophysical measurements, the swelling solvent was replaced with fresh solvent.

For variable-temperature fluorescence quantum yield measurements, the sample temperature was controlled with a water bath and an immersion heater. After the temperature of the water bath reached the target temperature, the quartz cells containing the samples were kept immersed in the water bath for 10 min. Then, their fluorescence quantum yields were measured (~10 s) quickly right after retrieving the samples from the water bath. For the measurement of the fluorescence spectra, the temperature of the sample solutions was controlled by a UNISOKU CoolSpeK USP-203 unit, which was mounted within a JASCO FP-6500 spectrofluorometer. The stirred sample solutions were also incubated for 10 min at the respective target temperatures.

Synthesis and characterization

9,10-Bis(*N*-(3-chloropropyl)-*N*-methylamino)anthracene (3). A solution of potassium *tert*-butoxide (2.0 g, 21 mmol), PEPPSI™-IPr catalyst (142 mg, 0.21 mmol), *N*-methyl-3-chloropropylamine hydrochloride (2, 1.3 g, 9.2 mmol), and 9,10-dibromoanthracene (1, 1.4 g, 4.2 mmol) in dry and degassed 1,4-dioxane (70 mL) was stirred at 100 °C for 18 h. After cooling to room temperature, the reaction mixture was filtered and the filtrate was extracted with ethyl acetate/hexane (1 : 2, v/v). The combined organic layers were washed with water and brine, before being dried over magnesium sulfate. The solvent was removed *in vacuo*, and the residue was purified by column chromatography on silica gel using dichloromethane/hexane (1 : 4, v/v) to yield crude **3** (1.4 g) as a yellow solid. The crude product was used for the next step of the reaction without further purification. Yield: 87%; ^{1}H NMR (300 MHz, $CDCl_3$): δ 8.33 (dd, $^4J = 3.3$ Hz, $^3J = 6.8$ Hz, 4H), 7.46 (dd, $^4J = 3.3$ Hz, $^3J = 6.8$ Hz, 4H), 3.64 (t, $^3J = 6.9$ Hz, 4H), 3.60 (t, $^3J = 6.5$ Hz, 4H), 3.22 (s, 6H), 2.03 (quint, $^3J = 6.8$ Hz, 4H) ppm (Fig. S1†).

9,10-Bis(*N*-(3-bromopropyl)-*N*-methylamino)anthracene (4). The reaction apparatus was flame-dried *in vacuo* before being charged under an argon atmosphere with a mixture of **3** (3.5 g, 9.0 mmol) and sodium bromide (0.37 g, 3.6 mmol). Subsequently, 1-methyl-2-pyrrolidine (50 mL) and 1-bromoethane (13 mL) were deaerated by sparging with argon and added to this mixture, which was then stirred for 31 h at 65 °C, before more 1-bromoethane (6.7 mL) was added. The reaction mixture was stirred for further 16 h at the same temperature. After complete consumption of **3** (monitored by TLC), the reaction mixture was extracted with ethyl acetate and washed with water and brine. The combined organic layers were dried over magnesium sulfate before the solvent was removed *in vacuo*. The thus obtained residue was purified by column chromatography on silica gel using chloroform : hexane (1 : 3, v/v) to yield crude **4** (3.5 g) as a yellow solid. Yield: 81%; ^{1}H NMR (300 MHz, $CDCl_3$):

δ 8.32 (dd, $^4J = 3.3$ Hz, $^3J = 6.8$ Hz, 4H), 7.46 (dd, $^4J = 3.3$ Hz, $^3J = 6.8$ Hz, 4H), 3.63 (t, $^3J = 6.9$ Hz, 4H), 3.45 (t, $^3J = 6.7$ Hz, 4H), 3.21 (s, 6H), 2.11 (quint, $^3J = 6.8$ Hz, 4H) ppm (Fig. S2†).

9,10-Bis((*N*-(3′-(*N*″-(3″-hydroxyprop-1″-yl)-*N*″-methylamino))prop-1′-yl)-*N*-methylamino)anthracene (6). A solution of **4** (0.50 g, 1.0 mmol), cesium carbonate (0.85 g, 2.6 mmol), and potassium iodide (0.17 g, 1.0 mmol) in deaerated acetonitrile was treated dropwise with 3-(*N*-methylamino)-1-propanol (**5**, 0.50 mL, 5.2 mmol). The reaction mixture was heated to reflux for 12 h under an atmosphere of argon. After cooling to room temperature, the reaction mixture was extracted with chloroform and the combined organic layers were washed with water and brine, before being dried over magnesium sulfate. Then, all volatiles were removed *in vacuo*. The residue was purified by column chromatography on silica gel using (i) hexane : chloroform (1 : 1, v/v), (ii) ethyl acetate, and (iii) ethyl acetate : methanol (5 : 1, v/v) with 5% triethylamine (v/v) to yield **6** (0.39 g) as a yellow solid. Yield: 76%; mp: 123.6–124.5 °C; ^{1}H NMR (500 MHz, $CDCl_3$): δ 8.34 (dd, $^4J = 3.3$ Hz, $^3J = 6.8$ Hz, 4H), 7.44 (dd, $^4J = 3.3$ Hz, $^3J = 6.8$ Hz, 4H), 3.71 (m, 4H), 3.49 (t, 4H, $^3J = 7.1$ Hz), 3.48 (s, 2H), 3.20 (s, 6H), 2.50 (t, 4H, $^3J = 5.8$ Hz), 2.40 (t, 4H, $^3J = 7.4$ Hz), 2.17 (s, 6H), 1.77 (quint, 4H, $^3J = 7.1$ Hz), 1.63–1.60 (m, 4H) ppm (Fig. S3†); ^{13}C NMR (125 MHz, $CDCl_3$): δ 143.3 (*Ar*), 131.4 (*Ar*), 125.6 (*Ar*), 124.6 (*Ar*), 64.6, 58.6, 56.2, 55.7, 50.8, 43.2, 41.9, 27.6 ppm (Fig. S4†); FT-IR (KBr): 3150 (OH), 1618 (Ar ring stretch), 1475 (Ar ring stretch), 1385 (Ar-N stretch), 776 (Ar-H) cm^{-1}. The structure of **6** was also supported by a NOESY spectrum (Fig. S15–S18†).

Methacrylate-monofunctionalized 9,10-bis((*N*-(3′-(*N*″-(3″-hydroxyprop-1″-yl)-*N*″-methylamino))prop-1′-yl)-*N*-methylamino) anthracene (ANTH-monomer). The reaction apparatus was flame-dried *in vacuo* before being charged with a solution of **6** (1.1 g, 2.1 mmol) and dry triethylamine (3.0 mL, 21 mmol) in deaerated and dry chloroform (30 mL). Methacryloyl chloride (0.23 mL, 2.4 mmol) was added to this solution at 0 °C, and the mixture was stirred under an argon atmosphere for 10 min before being allowed to warm to room temperature, where stirring was continued for 5 h. The reaction mixture was consecutively washed with aqueous sodium hydroxide (1 M, 100 mL), water, and brine. The combined organic layers were dried over magnesium sulfate, before all volatiles were removed *in vacuo*. The residue was purified by column chromatography on silica gel using (i) ethyl acetate and (ii) ethyl acetate : methanol (5 : 1, v/v) with 5% triethylamine (v/v), which afforded crude **ANTH-monomer** as a yellow liquid. Further purification was achieved by high-performance liquid chromatography (HPLC), which furnished pure **ANTH-monomer** (0.32 g). Yield: 26%; ^{1}H NMR (300 MHz, $CDCl_3$): δ 8.35 (dd, $^4J = 1.7$ Hz, $^3J = 4.2$ Hz, 2H), 8.33 (dd, $^4J = 1.7$ Hz, $^3J = 4.2$ Hz, 2H), 7.46–7.40 (m, 4H), 6.06 (dq, $^4J = 0.9$ Hz, $^3J = 1.7$ Hz, 1H), 5.51 (dq, $^4J = 1.5$ Hz, $^3J = 1.7$ Hz, 1H), 4.98 (brs, 1H), 4.12 (t, $^3J = 6.5$ Hz, 2H), 3.72 (t, $^3J = 5.3$ Hz, 2H), 3.49 (t, $^3J = 7.2$ Hz, 4H), 3.20 (s, 6H), 2.49 (t, $^3J = 5.7$ Hz, 2H), 2.38 (t, $^3J = 8.2$ Hz, 2H), 2.36 (t, $^3J = 7.9$ Hz, 4H), 2.17 (s, 3H), 2.14 (s, 3H), 1.92 (dd, $^4J = 0.9$ Hz, $^4J = 1.5$ Hz, 3H), 1.79–1.70 (m, 6H), 1.66–1.60 (m, 2H) ppm (Fig. S6†); ^{13}C NMR (75 MHz, $CDCl_3$): δ 167.3 (*C*O), 143.4 (*Ar*), 143.2 (*Ar*), 136.5 (*C*=*C*H$_2$), 131.4 (*Ar*), 131.4 (*Ar*), 125.6 (*Ar*), 125.5 (*Ar*), 125.1 (*C*=*C*H$_2$), 124.6 (*Ar*), 124.5 (*Ar*), 64.5, 63.1, 58.4, 56.2, 55.9, 55.8, 55.7, 54.3, 43.1, 43.1, 42.2, 41.9, 27.9, 27.7, 26.6, 18.2 ppm (Fig. S7†); FT-IR (neat): 2951, 1718 (C=O ester stretch), 1637 (Ar ring stretch), 1392 (Ar-N stretch), 779 (Ar-H) cm^{-1}; HRMS (FAB+) exact mass calculated for $[M + H]^+$ ($C_{34}H_{51}N_4O_3$): $m/z = 563.3961$, found: $m/z = 563.3965$.

Methacrylate-difunctionalized 9,10-bis((*N*-(3′-(*N*″-(3″-hydroxyprop-1″-yl)-*N*″-methylamino))prop-1′-yl)-*N*-methylamino) anthracene (ANTH-linker). The reaction apparatus was flame-dried *in vacuo* before being charged with a solution of **6** (0.50 g, 1.0 mmol) and dry trimethylamine (1.4 mL, 10 mmol) in deaerated and dry chloroform (30 mL). Under an argon atmosphere, methacryloyl chloride (0.29 mL, 3.0 mmol) was added at 0 °C, and the reaction mixture was stirred at this temperature for 10 min before being allowed to warm to room temperature, where stirring was continued for 5 h. After the complete consumption of **6** (monitored by TLC), the reaction mixture was consecutively washed with aqueous potassium hydroxide (1 M, 100 mL), water, and brine. The combined organic layers were dried over magnesium sulfate, before the solvent was removed *in vacuo*. The residue was purified by column chromatography on silica gel using ethyl acetate followed by ethyl acetate : methanol (5 : 1, v/v) to afford **ANTH-linker** (0.48 g) as a yellow liquid. Yield: 75%; ^{1}H NMR (300 MHz, $CDCl_3$): δ 8.34 (dd, $^4J = 3.2$ Hz, $^3J = 6.8$ Hz, 4H), 7.43 (dd, $^4J = 3.2$ Hz, $^3J = 6.8$ Hz, 4H), 6.07 (s, 2H), 5.53 (s, 2H), 4.12 (t, $^3J = 6.0$ Hz, 4H), 3.49 (t, $^3J = 7.1$ Hz, 4H), 3.19 (s, 6H), 2.42–2.37 (m, 8H), 2.18 (s, 6H), 1.92 (s, 6H), 1.79–1.75 (m, 8H) ppm (Fig. S8†); ^{13}C NMR (75 MHz, $CDCl_3$): δ 167.3 (*C*O), 143.3 (*Ar*), 136.3 (*C*=*C*H$_2$), 131.3 (*Ar*), 125.5 (*Ar*), 125.3 (*C*=*C*H$_2$), 124.6 (*Ar*), 62.9, 55.8, 55.5, 54.1, 43.0, 41.9, 27.5, 26.2, 18.3 ppm (Fig. S9†); FT-IR (neat): 2950, 1717 (C=O ester stretch), 1638 (Ar ring stretch), 1392 (Ar-N stretch), 779 (Ar-H) cm^{-1}; HRMS (FAB+) exact mass calculated for $[M + H]^+$ ($C_{38}H_{55}N_4O_4$): $m/z = 631.4223$, found: $m/z = 631.4210$.

1,4-Dibromo-2,3-dimethylnaphthalene (9).[38] A stirred solution of 2,3-dimethylnaphthalene (1.0 g, 6.4 mmol) in chloroform (10 mL) at 0 °C was gradually treated with a solution of bromine (0.69 mL, 13 mmol) in chloroform (6 mL). The reaction mixture was stirred for 10 min at 0 °C, before being allowed to warm to room temperature. The reaction mixture was set aside for 3 h before being quenched by addition of sodium thiosulfate monohydrate (5.5 g, 19 mmol). The resultant suspension was extracted with chloroform and the combined organic layers were washed with water and brine. Then, the organic fraction was dried over magnesium sulfate and the solvent was removed *in vacuo* to yield crude **9** (2.0 g) as a white solid. Yield: ≥99%; ^{1}H NMR (300 MHz, $CDCl_3$): δ 8.30 (dd, $^4J = 3.4$ Hz, $^3J = 6.3$ Hz, 2H), 7.54 (dd, $^4J = 3.4$ Hz, $^3J = 6.3$ Hz, 2H), 2.69 (s, 6H) ppm (Fig. S10†).

5-(*tert*-Butyldiphenylsiloxy)pentan-1-amine (11). At 0 °C, a stirred solution of 5-amino-1-pentanol (**10**; 2.9 g, 28 mmol) and imidazole (2.8 g, 41 mmol) in dichloromethane (50 mL) was treated dropwise with *tert*-butyldiphenylchlorosilane (8.5 mL, 33 mmol). After the exothermic stopped, the reaction temperature was allowed to raise to room temperature, where stirring was continued for 5 h, before the temperature was raised to

40 °C, were stirring was continued for 1 h. The reaction was quenched with water and washed with brine. The combined organic layers were dried over magnesium sulfate and the solvent was removed *in vacuo*. The residue was purified by column chromatography on silica gel consecutively using ethyl acetate : hexane (1 : 1, v/v) and ethyl acetate : methanol (5 : 1, v/v) with 5% triethylamine to afford crude **11** (6.8 g) as a colorless liquid. Yield: 72%; ^{1}H NMR (300 MHz, $CDCl_3$): δ 7.66 (dd, ^4J = 1.9 Hz, ^3J = 7.4 Hz, 4H), 7.40–7.33 (m, 6H), 4.29 (brs, 2H), 3.65 (t, ^3J = 6.3 Hz, 2H), 2.75 (t, ^3J = 7.2 Hz, 2H), 1.59–1.49 (m, 4H), 1.41–1.36 (m, 2H), 1.05 (s, 9H) ppm (Fig. S11†).

1,4-Bis(*N*-(5-(*tert*-butyldiphenylsiloxy)-pent-1-yl)amino)-2,3-dimethylnaphthalene (12). A solution of sodium *tert*-butoxide (1.5 g, 16 mmol), PEPPSI™-IPr catalyst (0.13 g, 0.19 mmol), 5-(*tert*-butyldiphenylsiloxy)pentan-1-amine (**11**; 2.7 g, 8.0 mmol), and 1,4-dibromo-2,3-dimethylnaphthalene (**9**; 1.0 g, 3.2 mmol) in deaerated and dry 1,4-dioxane (100 mL) was stirred for 15 min under argon at room temperature. The resulting mixture was heated to reflux for 72 h. After cooling to room temperature, the reaction mixture was extracted with ethyl acetate and the combined organic layers were washed with water and brine. Then, the organic layer was dried over magnesium sulfate and the solvent was removed *in vacuo*. The residue was purified by column chromatography on silica gel using hexane : ethyl acetate (10 : 1, v/v) to afford crude **12** (2.1 g) as a pale yellow liquid. Yield: 80%; ^{1}H NMR (300 MHz, $CDCl_3$): δ 8.03 (dd, ^4J = 3.4 Hz, ^3J = 6.4 Hz, 2H, ArH), 7.72–7.66 (m, 8H, ArH), 7.40–7.31 (m, 14H, ArH), 3.69 (t, ^3J = 6.2 Hz, 4H, CH_2), 3.10 (brs, 2H, NH), 2.98 (t, ^3J = 7.0 Hz, 4H, CH_2), 2.36 (s, 6H, $ArCH_3$), 1.67–1.61 (m, 8H, CH_2), 1.54–1.52 (m, 4H, CH_2), 1.06 (s, 18H, $C(CH_3)_3$) ppm (Fig. S12†).

1,4-Bis(*N*-(5-(*tert*-butyldiphenylsiloxy)-pent-1-yl)-*N*-methylamino)-2,3-dimethylnaphthalene (13). A solution of **12** (0.96 g, 1.2 mmol) and sodium carbonate (0.31 g, 2.9 mmol) in deaerated acetonitrile (30 mL) was treated at room temperature with methyl iodide (0.22 mL, 3.5 mmol). The reaction mixture was warmed to 60 °C and stirred for 12 h under argon. Then, more methyl iodide (0.22 mL, 3.5 mmol) was added and the reaction mixture was stirred for 4 h at the same temperature. After the complete consumption of **12** (monitored by TLC), the reaction mixture was extracted with ethyl acetate and the combined organic layers were washed with water and brine. Then, the organic layer was dried over magnesium sulfate and the solvent was removed *in vacuo*. The thus obtained residue was purified by column chromatography on silica gel using hexane : ethyl acetate (20 : 1, v/v) to afford crude **13** (0.84 g) as a colorless liquid. Crude **13** was used in the next reaction step without further purification. Yield: 85%; ^{1}H NMR (300 MHz, $CDCl_3$): δ 8.13 (dd, ^4J = 3.3 Hz, ^3J = 6.1 Hz, 2H), 7.66 (dd, ^4J = 2.0 Hz, ^3J = 7.6 Hz, 8H), 7.37–7.31 (m, 14H), 3.64 (t, ^3J = 6.4 Hz, 4H), 3.18–3.13 (m, 4H), 2.93 (s, 6H), 2.32 (s, 6H), 1.58–1.53 (m, 8H), 1.42–1.38 (m, 4H), 1.04 (s, 18H) ppm (Fig. S13†).

1,4-Bis(*N*-(hydroxypent-5-yl)-*N*-methylamino)-2,3-dimethylnaphthalene (14). A solution of TBDPS-protected alcohol **13** (1.4 g, 1.6 mmol) in dry THF (30 mL) was treated with a THF solution of tetrabutylammonium fluoride (6.4 mL, 1 M, 6.4 mmol). The reaction mixture was stirred for 21 h under argon at room temperature. After the complete consumption of **13** (monitored by TLC), the reaction mixture was extracted with ethyl acetate and the combined organic layers were washed with water and brine. Then, the organic layer was dried over magnesium sulfate and the solvent was removed *in vacuo*. The residue was purified by column chromatography on silica gel using hexane : ethyl acetate (1 : 1, v/v) to afford crude **14** (0.59 g) as a colorless liquid. For further purification, column chromatography on silica gel was repeated. Yield: 95%; ^{1}H NMR (500 MHz, $CDCl_3$): δ 8.13 and 8.13 (dd, ^4J = 3.3 Hz, ^3J = 6.4 Hz, 2H, Ar*H* of different rotamers), 7.37 (dd, ^4J = 3.3 Hz, ^3J = 6.4 Hz, 2H, Ar*H*), 3.59 and 3.56 (t, ^3J = 6.6 Hz, 4H, CH_2 of different rotamers), 3.18 and 3.17 (t, ^3J = 6.9 Hz, 4H, CH_2 of different rotamers), 2.95 and 2.94 (s, 6H, NCH_3 of different rotamers), 2.33 and 2.33 (s, 6H, $ArCH_3$ of different rotamers), 1.66 (brs, 2H, O*H*), 1.59–1.49 (m, 8H, CH_2), 1.39–1.33 (m, 4H, CH_2) ppm (Fig. S14†); ^{13}C NMR (125 MHz, $CDCl_3$): δ 143.8 and 143.7 (*Ar* of different rotamers), 135.0 and 134.9 (*Ar* of different rotamers), 132.4 (*Ar*), 124.8 (*Ar*), 124.2 (*Ar*), 62.8 and 62.7 (CH_2 of different rotamers), 56.7 and 56.6 (CH_2 of different rotamers), 41.6 and 41.5 (NCH_3 of different rotamers), 32.6 and 32.5 (CH_2 of different rotamers), 29.4 and 29.4 (CH_2 of different rotamers), 23.4 and 23.3 (CH_2 of different rotamers), 16.2 and 16.2 ($ArCH_3$ of different rotamers) ppm (Fig. S15†); HRMS (FAB+) exact mass calculated for $[M]^+$ ($C_{24}H_{38}N_2O_2$): m/z = 386.2933, found: m/z = 386.2937. These ^{1}H and ^{13}C NMR signals were assigned on the basis of DEPT-135, ^{1}H–^{1}H COSY, ^{1}H–^{13}C HSQC, and NOESY spectra (Fig. S5†).

Methacrylate-monofunctionalized 1,4-bis(*N*-(hydroxypent-5-yl)-*N*-methylamino)-2,3-dimethylnaphthalene (NAPH-monomer). The reaction apparatus was flame-dried *in vacuo* before a stirred solution of **14** (0.50 g, 1.3 mmol) and dry triethylamine (1.8 mL, 13 mmol) in deaerated and dry chloroform (18 mL) was treated at 0 °C with methacryloyl chloride (0.14 mL, 1.4 mmol). Under an argon atmosphere, the reaction mixture was stirred at this temperature for 10 min, before being allowed to warm to room temperature, where stirring was continued for 3 h. After the complete consumption of **14** (monitored by TLC), the reaction mixture was washed consecutively with aqueous potassium hydroxide (1 M, 100 mL), water, and brine. The combined organic layers were dried over magnesium sulfate before the solvent was removed *in vacuo*. The residue was purified by column chromatography on silica gel using ethyl acetate : hexane (1 : 1, v/v) to afford **NAPH-monomer** (0.25 g) as a colorless liquid. The **NAPH-monomer** was thoroughly purified by column chromatography on silica gel using chloroform as the eluent immediately prior to any photophysical measurements and polymerization reactions. Yield: 43%; ^{1}H NMR (500 MHz, $CDCl_3$): δ 8.13 and 8.12 (dd, ^4J = 3.3 Hz, ^3J = 6.5 Hz, 2H, Ar*H* of different rotamers), 7.37 (dd, ^4J = 3.3 Hz, ^3J = 6.5 Hz, 2H, Ar*H*), 6.06 (s, 1H, C=CH_2), 5.52 (s, 1H, C=CH_2), 4.11 and 4.10 (t, ^3J = 6.5 Hz, 2H, CH_2 of different rotamers), 3.57 (t, ^3J = 6.5 Hz, 2H, CH_2), 3.22–3.15 (m, 4H, CH_2 of different rotamers), 2.94 and 2.93 (s, 6H, NCH_3 of different rotamers), 2.33 and 2.33 (s, 6H, $ArCH_3$ of different rotamers), 1.91 (s, 3H, $COC(CH_3)$), 1.66–1.49 (m, 8H, CH_2 of different rotamers), 1.41–1.34 (m, 4H, CH_2 of different rotamers) ppm (Fig. S19†); ^{13}C NMR (125 MHz,

$CDCl_3$): δ 167.5 (*C*O), 143.9 and 143.9 (*Ar* of different rotamers), 143.8 (*Ar*), 143.8 (*Ar*), 136.4 (*C*=*C*H_2), 135.0 and 135.0 (*Ar* of different isomers), 135.0 (*Ar*), 132.4 (*Ar*), 132.4 and 132.4 (*Ar* of different rotamers), 125.2 (*C*=*C*H_2), 124.8 (*Ar*), 124.7 (*Ar*), 124.2 and 124.2 (*Ar* of different rotamers), 64.8, 62.8, 56.7, 56.6, 41.5, 41.5, 32.6, 29.5, 29.4, 28.5, 23.8, 23.4, 18.3, 16.3, 16.2 ppm (Fig. S20†); FT-IR (neat): 2933, 1718 (C=O ester stretch), 1637 (Ar ring stretch), 1577, 1387 (Ar-N stretch), 756 (Ar-H) cm^{-1}; HRMS (FAB+) exact mass calculated for $[M]^+$ ($C_{28}H_{42}N_2O_3$): m/z = 454.3195, found: m/z = 454.3195.

Methacrylate-difunctionalized 1,4-bis(*N*-(hydroxypent-5-yl)-*N*-methylamino)-2,3-dimethylnaphthalene (NAPH-linker). The reaction apparatus was flame-dried *in vacuo* before a stirred solution of **14** (0.31 g, 0.81 mmol) and dry triethylamine (1.1 mL, 7.8 mmol) in deaerated and dry chloroform (11 mL) was treated at 0 °C with methacryloyl chloride (0.24 mL, 2.4 mmol). Under an argon atmosphere, the reaction mixture was stirred at this temperature for 10 min, before being allowed to warm to room temperature, where stirring was continued for 3 h. After complete consumption of **14** (monitored by TLC), the reaction mixture was consecutively washed with aqueous potassium hydroxide (1 M, 100 mL), water, and brine. The combined organic layers were dried over magnesium sulfate before the solvent was removed *in vacuo*. The thus obtained residue was purified by column chromatography on silica gel using ethyl acetate : hexane (1 : 4, v/v) to afford **NAPH-linker** (0.42 g) as a colorless liquid. Immediately prior to any photophysical measurements and polymerization reactions, the **NAPH-linker** was thoroughly purified by column chromatography on silica gel using chloroform as the eluent. Yield: 99%; ^{1}H NMR (300 MHz, $CDCl_3$): δ 8.12 (dd, ^4J = 3.3 Hz, ^3J = 6.5 Hz, 2H, Ar*H*), 7.37 (dd, ^4J = 3.3 Hz, ^3J = 6.5 Hz, 2H, Ar*H*), 6.06 (s, 2H, C=CH_2), 5.51 (s, 2H, C=CH_2), 4.11 (t, ^3J = 6.6 Hz, 4H, CH_2), 3.20 and 3.18 (two triplets from different isomers, ^3J = 7.0 Hz, 4H, CH_2), 2.94 (s, 6H, NCH_3), 2.33 (s, 6H, ArCH_3), 1.92 (s, 6H, COC(CH_3)), 1.66 (quint, ^3J = 6.9 Hz, 4H, CH_2), 1.59 (quint, ^3J = 7.3 Hz, 4H, CH_2), 1.45–1.36 (m, 4H, CH_2) ppm (Fig. S21†); ^{13}C NMR (75 MHz, $CDCl_3$): δ 167.3 (*C*O), 144.7 (*Ar*), 137.5 (*C*=*C*H_2), 135.7 and 135.7 (*Ar* from different isomers), 133.3 (*Ar*), 125.5 (*C*=*C*H_2), 125.3 (*Ar*), 125.1 (*Ar*), 65.1, 57.4, 41.8, 30.6, 30.2, 24.5, 18.4, 16.5 and 16.4 (from different isomers) ppm (Fig. S22†); FT-IR (neat): 2936, 1717 (C=O ester stretch), 1638 (Ar ring stretch), 1387 (Ar-N stretch), 757 (Ar-H) cm^{-1}; HRMS (FAB+) exact mass calculated for $[M]^+$ ($C_{32}H_{46}N_2O_4$): m/z = 522.3458, found: m/z = 522.3460.

Representative co-polymerization procedure

A 10 mL Schlenk tube with a stopcock in the sidearm was flame-dried in *vacuo* before being charged with *N*-isopropyl acrylamide (NIPAM) (1.13 g, 10.0 mmol), a solution of **NAPH-monomer** (5.0×10^{-2} M, 3.6 mL for a monomer feed ratio $x : y$ = 56 : 1, 2.4 mL for $x : y$ = 83 : 1, and 1.2 mL for $x : y$ = 167 : 1), and 2,2′-azobisisobutyronitrile (AIBN, 16 mg, 0.10 mmol). Then, dry, deaerated THF was added under an argon atmosphere to reach a total volume of 5 mL for the reaction mixture. Subsequently, the reaction mixture was subjected to thorough argon sparging until the total volume of the reaction mixture decreased to 4 mL. The reaction mixture was kept for 20 h at 55 °C, before being transferred into diethyl ether at 0 °C. The thus obtained precipitate was collected by filtration and dissolved again in THF. This reprecipitation procedure was repeated three times to afford **[ANTH-polymer]$_x$** and **[NAPH-polymer]$_x$** as yellow and colorless solids, respectively. Yields for **[ANTH-polymer]$_x$**: 75% (0.85 g) for $x : y$ = 56 : 1, 61% (0.69 g) for $x : y$ = 83 : 1, 84% (0.95 g) for $x : y$ = 167 : 1; yields for **[NAPH-polymer]$_x$**: 91% (1.0 g) for $x : y$ = 56 : 1, 96% (1.1 g) for $x : y$ = 83 : 1, 95% (1.1 g) for $x : y$ = 167 : 1; ^{1}H NMR (500 MHz, $CDCl_3$): δ 6.80–6.20 (br, 1H, CON*H*), 4.00 (m, 1H, C*H*(CH_3)$_2$), 2.14 (m, 1H, C*H*CH_2), 1.86–1.35 (m, 2H, CHCH_2), 1.14 (m, 6H, CH(CH_3)$_2$) ppm.[41] For a detailed assignment, see Fig. S23 and S24.†

Representative procedure for the preparation of gels

A 10 mL Schlenk tube with a stopcock in the sidearm was flame-dried *in vacuo* before *N*-isopropyl acrylamide (NIPAM, 1.13 g, 10.0 mmol), a THF solution of **ANTH-linker** (5.0×10^{-2} M, 3.6 mL for a monomer feed ratio $x : y$ = 56 : 1, 2.4 mL for $x : y$ = 83 : 1, 1.2 mL for $x : y$ = 167 : 1), and 2,2′-azobisisobutyronitrile (AIBN, 16 mg, 0.10 mmol) were added. Dry, deaerated THF was added under an argon atmosphere to reach a total volume of 5 mL for the reaction mixture. Then, the reaction mixture was subjected to thorough argon sparging until the total volume of the reaction mixture decreased to 4 mL. The reaction mixture was kept at 55 °C for 20 h, before being transferred to THF (150 mL) in order to confirm the formation of a gel. The thus prepared PNIPAM gel was purified by Soxhlet extraction using THF as eluents to afford yellow (**[ANTH-gel]$_x$**) or colorless (**[NAPH-gel]$_x$**) gels.

References

1 M. A. Haidekker and E. A. Theodorakis, *Org. Biomol. Chem.*, 2007, **5**, 1669–1678.
2 N. Amdursky, Y. Erez and D. Huppert, *Acc. Chem. Res.*, 2012, **45**, 1548–1557.
3 L. Zhu and Y. Zhao, *J. Mater. Chem. C*, 2013, **1**, 1059–1065.
4 T. Liu, X. Liu, D. R. Spring, X. Qian, J. Cui and Z. Xu, *Sci. Rep.*, 2014, **4**, 5418.
5 (*a*) M. K. Kuimova, G. Yahioglu, J. A. Levit and K. Suhling, *J. Am. Chem. Soc.*, 2008, **130**, 6672–6673; (*b*) M. K. Kuimova, S. W. Botchway, A. W. Parker, M. Balaz, H. A. Collins, H. L. Anderson, K. Suhling and P. R. Ogilby, *Nat. Chem.*, 2009, **1**, 69–73; (*c*) V. I. Stsiapura, A. A. Maskevich, V. A. Kuzmitsky, V. N. Uversky, I. M. Kuznetsova and K. K. Turoverov, *J. Phys. Chem. B*, 2008, **112**, 15893–15902; (*d*) M. Nishikawa, S. Kume and H. Nishihara, *Phys. Chem. Chem. Phys.*, 2013, **15**, 10549–10565; (*e*) G. Vaccaro, A. Bianchi, M. Mauri, S. Bonetti, F. Meinardi, A. Sanguineti, R. Simonutti and L. Beverina, *Chem. Commun.*, 2013, **49**, 8474–8476; (*f*) I. A. Karpenko, Y. Niko, V. P. Yakubovskyi, A. O. Gerasov, D. Bonnet, Y. P. Kovtun and A. S. Klymchenko, *J. Mater. Chem. C*, 2016, **4**, 3002–

3009; (*g*) A. S. Klymchenko, *Acc. Chem. Res.*, 2017, **50**, 366–375.

6 (*a*) J. Mei, Y. Hong, J. W. Y. Lam, A. Qin, Y. Tang and B. Z. Tang, *Adv. Mater.*, 2014, **26**, 5429–5479; (*b*) J. Mei, N. L. C. Leung, R. T. K. Kwok, J. W. Y. Lam and B. Z. Tang, *Chem. Rev.*, 2015, **115**, 11718–11940; (*c*) R. T. K. Kwok, C. W. T. Leung, J. W. Y. Lam and B. Z. Tang, *Chem. Soc. Rev.*, 2015, **44**, 4228–4238; (*d*) Y. Hong, J. W. Y. Lam and B. Z. Tang, *Chem. Soc. Rev.*, 2011, **40**, 5361–5388; (*e*) S. Sasaki, G. P. C. Drummen and G. Konishi, *J. Mater. Chem. C*, 2016, **4**, 2731–2743; (*f*) Y. Niko and G. Konishi, *J. Synth. Org. Chem., Jpn.*, 2012, **70**, 918–927.

7 (*a*) H. Naito, Y. Morisaki and Y. Chujo, *Angew. Chem., Int. Ed.*, 2015, **54**, 5084–5087; (*b*) C. Botta, S. Benedini, L. Carlucci, A. Forni, D. Marinotto, A. Nitti, D. Pasini, S. Righetto and E. Cariati, *J. Mater. Chem. C*, 2016, **4**, 2979–2989; (*c*) H. Zhou, Q. Ye, X. Y. Wu, J. Song, C. M. Cho, Y. Zong, B. Z. Tang, T. S. A. Hor, E. K. L. Yeow and J. W. Xu, *J. Mater. Chem. C*, 2015, **3**, 11874–11880; (*d*) R. Yoshii, K. Suenaga, K. Tanaka and Y. Chujo, *Chem.–Eur. J.*, 2015, **21**, 7231–7237; (*e*) H. Imoto, K. Nohmi, K. Kizaki, S. Watase, K. Matsukawa, S. Yamamoto, M. Mitsuishi and K. Naka, *RSC Adv.*, 2015, **5**, 94344–94350; (*f*) H. Imoto, K. Kizaki, S. Watase, K. Matsukawa and K. Naka, *Chem.–Eur. J.*, 2015, **21**, 12105–12111; (*g*) J. Li, W. Yang, W. Q. Zhou, C. C. Li, Z. Q. Cheng, M. Y. Li, L. Q. Xie and Y. Y. Li, *RSC Adv.*, 2016, **6**, 35833–35841; (*h*) Q. K. Sun, W. Liu, S. A. Ying, L. L. Wang, S. F. Xue and W. J. Yang, *RSC Adv.*, 2015, **5**, 73046–73050; (*i*) T. Jiang, Y. Qu, B. Li, Y. T. Gao and J. L. Hua, *RSC Adv.*, 2015, **5**, 1500–1506; (*j*) T. Jadhav, B. Dhokale, S. M. Mobin and R. Misra, *RSC Adv.*, 2015, **5**, 29878–29884.

8 (*a*) J. Liang, B. Z. Tang and B. Liu, *Chem. Soc. Rev.*, 2015, **44**, 2798–2811; (*b*) J. Yang, N. Sun, J. Huang, Q. Q. Li, Q. Peng, X. Tang, Y. Q. Dong, D. G. Ma and Z. Li, *J. Mater. Chem. C*, 2015, **3**, 2624–2631; (*c*) Y. Okazawa, K. Kondo, M. Akita and M. Yoshizawa, *J. Am. Chem. Soc.*, 2015, **137**, 98–101; (*d*) R. Y. Zhang, R. T. K. Kwok, B. Z. Tang and B. Liu, *RSC Adv.*, 2015, **5**, 28332–28337; (*e*) D. Belei, C. Dumea, E. Bicu and L. Marin, *RSC Adv.*, 2015, **5**, 8849–8858; (*f*) Z. F. Huang, X. Q. Zhang, X. Y. Zhang, C. K. Fu, K. Wang, J. Y. Yuan, L. Tao and Y. Wei, *Polym. Chem.*, 2015, **6**, 607–612; (*g*) Z. Chen, X. Han, J. Zhang, D. Wu, G. A. Yu, J. Yin and S. H. Liu, *RSC Adv.*, 2015, **5**, 15341–15349; (*h*) Q. Wan, K. Wang, H. L. Du, H. Y. Huang, M. Y. Liu, F. J. Deng, Y. F. Dai, X. Y. Zhang and Y. Wei, *Polym. Chem.*, 2015, **6**, 5288–5294; (*i*) H. Yamane, S. Ito, K. Tanaka and Y. Chujo, *Polym. Chem.*, 2016, **7**, 2799–2807; (*j*) A. Pandith, A. Kumar and H. S. Kim, *RSC Adv.*, 2016, **6**, 68627–68637; (*k*) S. Sasaki, Y. Niko, K. Igawa and G. Konishi, *RSC Adv.*, 2014, **4**, 33474–33477.

9 (*a*) C. E. Kung and J. K. Reed, *Biochemistry*, 1989, **28**, 6678–6686; (*b*) S. Sawada, T. Iio, Y. Hayashi and S. Takahashi, *Anal. Biochem.*, 1992, **204**, 110–117.

10 (*a*) W. L. Goh, M. Y. Lee, T. L. Joseph, S. T. Quah, C. J. Brown, C. Verma, S. Brenner, F. J. Ghadessy and Y. N. Teo, *J. Am. Chem. Soc.*, 2014, **136**, 6159–6162; (*b*) M. A. Haidekker, T. Brady, K. Wen, C. Okada, H. Y. Stevens, J. M. Snell, J. A. Frangos and E. A. Theodorakis, *Bioorg. Med. Chem.*, 2002, **10**, 3627–3636; (*c*) T. Iwaki, C. Torigoe, M. Noji and M. Nakanishi, *Biochemistry*, 1993, **32**, 7583–7592; (*d*) K. Cao, M. Farahi, M. Dakanali, W. M. Chang, C. J. Sigurdson, E. A. Theodorakis and J. Yang, *J. Am. Chem. Soc.*, 2012, **134**, 17338–17341.

11 (*a*) R. O. Loutfy, *Pure Appl. Chem.*, 1986, **58**, 1239–1248; (*b*) S. K. Dishari and M. A. Hickner, *Macromolecules*, 2013, **46**, 413–421; (*c*) R. D. Priestley, P. Rittigstein, L. J. Broadbelt, K. Fukao and J. M. Torkelson, *J. Phys.: Condens. Matter*, 2007, **19**, 205120.

12 (*a*) R. D. Priestley, C. J. Ellison, L. J. Broadbelt and J. M. Torkelson, *Science*, 2005, **309**, 456–459; (*b*) M. K. Mundra, S. K. Donthu, V. P. Dravid and J. M. Torkelson, *Nano Lett.*, 2007, **7**, 713–718.

13 T. Suhina, B. Weber, C. E. Carpentier, K. Lorincz, P. Schall, D. Bonn and A. M. Brouwer, *Angew. Chem., Int. Ed.*, 2015, **54**, 3688–3691.

14 A. Mustafic, H.-M. Huang, E. A. Theodorakis and M. A. Haidekker, *J. Fluoresc.*, 2010, **20**, 1087–1098.

15 Y. Dong, J. W. Y. Lam, A. Qin, J. Sun, J. Liu, Z. Li, S. Zhang, J. Sun, H. S. Kwok and B. Z. Tang, *Appl. Phys. Lett.*, 2007, **91**, 011111.

16 The applications of functionalized TPE are too widespread in order to be covered exhaustively herein. Therefore, only selected examples are given here; for further details, see: ref. 6. (*a*) N. B. Shustova, B. D. McCarthy and M. Dinca, *J. Am. Chem. Soc.*, 2011, **133**, 20126–20129; (*b*) F. Ishiwari, H. Hasebe, S. Matsumura, F. Hajjaj, N. H. Hayashi, M. Nishi, T. Someya and T. Fukushima, *Sci. Rep.*, 2016, **6**, 24275; (*c*) X. Xue, Y. Zhao, L. Dai, X. Zhang, X. Hao, C. Zhang, S. Huo, J. Liu, C. Liu, A. Kumar, W.-Q. Chen, G. Zou and X.-J. Liang, *Adv. Mater.*, 2014, **26**, 712–717; (*d*) Y. Yuan, R. T. K. Kwok, R. Zhang, B. Z. Tang and B. Liu, *Chem. Commun.*, 2014, **50**, 11465–11468.

17 B. Z. Tang, *"Organic, Organometallic, and Metallic Luminogens" in Cutting-Edge Chemistry*, ACS, 15 Aug 2016, https://www.acs.org/content/acs/en/pressroom/cutting-edge-chemistry/organic-organometallic-and-metallic-luminogens.html.

18 S. Sasaki, S. Suzuki, W. M. C. Sameera, K. Igawa, K. Morokuma and G. Konishi, *J. Am. Chem. Soc.*, 2016, **138**, 8194–8206.

19 S. Sasaki, K. Igawa and G. Konishi, *J. Mater. Chem. C*, 2015, **3**, 5940–5950.

20 Y. Suzuki, N. Fukui, K. Murakami, H. Yorimitsu and A. Osuka, *Asian J. Org. Chem.*, 2013, **2**, 1066–1071.

21 (*a*) W. Huang and S. L. Buchwald, *Chem.–Eur. J.*, 2016, **22**, 14186–14189; (*b*) S. Riedmüller, O. Kaufhold, H. Spreitzer and B. J. Nachtsheim, *Eur. J. Org. Chem.*, 2014, 1391–1394; (*c*) M. Prashad, X. Y. Mak, Y. Liu and O. Repic, *J. Org. Chem.*, 2003, **68**, 1163–1164; (*d*) S. M. Raders, J. N. Moore, J. K. Parks, A. D. Miller, T. M. Leißing, S. P. Kelley, R. D. Rogers and K. H. Shaughnessy, *J. Org. Chem.*, 2013, **78**, 4649–4664; (*e*) G. L. Duc, S. Meiries and S. P. Nolan, *Organometallics*, 2013, **32**, 7547–7551.

22 (*a*) K. Kubota, S. Fujishige and I. Ando, *Polym. J.*, 1990, **22**, 15–20; (*b*) M. Heskins and J. E. Guillet, *J. Macromol. Sci., Part A: Pure Appl. Chem.*, 1968, **2**, 1441–1455.

23 (*a*) K. Okabe, N. Inada, C. Gota, Y. Harada, T. Funatsu and S. Uchiyama, *Nat. Commun.*, 2012, **3**, 705; (*b*) C. Gota, K. Okabe, T. Funatsu, Y. Harada and S. Uchiyama, *J. Am. Chem. Soc.*, 2009, **131**, 2766–2767; (*c*) C. D. S. Brites, P. P. Lima, N. J. O. Silva, A. Millan, V. S. Amaral, F. Palacio and L. D. Carlos, *Nanoscale*, 2012, **4**, 4799–4829.

24 F. M. Winnik, *Macromolecules*, 1990, **23**, 233–242.

25 C.-Y. Chen and C.-T. Chen, *Chem. Commun.*, 2011, **47**, 994–996.

26 E. M. Graham, K. Iwai, S. Uchiyama, A. P. De Silva, S. W. Magennis and A. C. Jones, *Lab Chip*, 2010, **10**, 1267–1273.

27 Y. Shiraishi, R. Miyamoto, X. Zhang and T. Hirai, *Org. Lett.*, 2007, **9**, 3921–3924.

28 D. Wang, R. Miyamoto, Y. Shiraishi and T. Hirai, *Langmuir*, 2009, **25**, 13176–13182.

29 M. C. Harris, X. Huang and S. L. Buchwald, *Org. Lett.*, 2002, **4**, 2885–2888.

30 A. Shafir, P. A. Lichtor and S. L. Buchwald, *J. Am. Chem. Soc.*, 2007, **129**, 3490–3491.

31 A. Shafir and S. L. Buchwald, *J. Am. Chem. Soc.*, 2006, **128**, 8742–8743.

32 J. Clayden, N. Greeves and S. Warren, *Organic Chemistry*, Oxford University Press, New York, 2nd edn, 2012, pp. 694–722.

33 (*a*) R. S. Coleman and W. Chen, *Org. Lett.*, 2001, **3**, 1141–1144; (*b*) K. Lakshman, J. C. Keeler, J. H. Hilmer and J. Q. Martin, *J. Am. Chem. Soc.*, 1999, **121**, 6090–6091.

34 O. J. Plante, S. L. Buchwald and P. H. Seeberger, *J. Am. Chem. Soc.*, 2000, **122**, 7148–7149.

35 (*a*) M. G. Organ, S. Calimsiz, M. Sayah, K. H. Hoi and A. J. Lough, *Angew. Chem., Int. Ed.*, 2009, **48**, 2383–2387; (*b*) C. Valente, S. Calimsiz, K. H. Hoi, D. Mallik, M. Sayah and M. G. Organ, *Angew. Chem., Int. Ed.*, 2012, **51**, 3314–3332.

36 T. W. Campbell, V. E. Mccoy, J. C. Kauer and V. S. Foldi, *J. Org. Chem.*, 1961, **26**, 1422–1426.

37 W. E. Willy, D. R. Mckean and B. A. Garcia, *Bull. Chem. Soc. Jpn.*, 1976, **49**, 1989–1995.

38 P. H. Gore, C. K. Thadani and S. Thorburn, *J. Chem. Soc. C*, 1968, 2502–2508.

39 R. A. Al-Horani and U. R. Desai, *Tetrahedron*, 2012, **68**, 2027–2040.

40 D. X. Hu, P. Grice and S. V. Ley, *J. Org. Chem.*, 2012, **77**, 5198–5202.

41 (*a*) M. Ito and T. Ishizone, *J. Polym. Sci., Part A: Polym. Chem.*, 2006, **44**, 4832–4845; (*b*) C. S. Biswas, V. K. Patel, N. K. Vishwakarma, V. K. Tiwari, B. Maiti, P. Maiti, M. Kamigaito, Y. Okamoto and B. Ray, *Macromolecules*, 2011, **44**, 5822–5824.

42 Z. Wang, Z. Yang, T. Gao, J. He, L. Gong, Y. Lu, Y. Xiong and W. Xu, *Anal. Methods*, 2015, **7**, 2738–2746.

43 F. M. Winnik, M. F. Ottaviani, S. H. Bossmann, W. Pan, M. Garcia-Garibay and N. J. Turro, *Macromolecules*, 1993, **26**, 4577–4585.

44 J. Hao, H. Cheng, P. Butler, L. Zhang and C. C. Han, *J. Chem. Phys.*, 2010, **132**, 154902.

45 H. Ringsdorf, J. Venzmer and F. M. Winnik, *Macromolecules*, 1991, **24**, 1678–1686.

46 F. M. Winnik, M. F. Ottaviani, S. H. Bossman, W. Pan, M. Garcia-Garibay and N. J. Turro, *J. Phys. Chem.*, 1993, **97**, 12998–13005.

47 M. Montalti, A. Credi, L. Prodi and M. T. Gandolfi, *Handbook of Photochemistry*, Taylor & Francis, Boca Raton, 2006, p. 548.

48 L. Tang, J. K. Jin, A. Qin, W. Z. Yuan, Y. Mao, J. Mei, J. Z. Sun and B. Z. Tang, *Chem. Commun.*, 2009, 4974–4976.

49 M. Onoda, S. Uchiyama and T. Ohwada, *Macromolecules*, 2007, **40**, 9651–9657.

50 K. Iwai, Y. Matsumura, S. Uchiyama and A. P. De Silva, *J. Mater. Chem.*, 2005, **15**, 2796–2800.

51 T. Li, S. He, J. Qu, H. Wu, S. Wu, Z. Zhao, A. Qin, R. Hu and B. Z. Tang, *J. Mater. Chem. C*, 2016, **4**, 2964–2970.

52 S. Uchiyama, Y. Matsumura, A. P. De Silva and K. Iwai, *Anal. Chem.*, 2003, **75**, 5926–5935.

53 S. Fujishige, K. Kubota and I. Ando, *J. Phys. Chem.*, 1989, **93**, 3311–3313.

